



A novel tool for pneumatic spindle design

M. Carfagni^(a), R. Furferi^(a), Y. Volpe^(a)

^(a) Dipartimento di Meccanica e Tecnologie Industriali, Università degli Studi di Firenze

Article Information

Keywords:

Spindle design,
Air motor,
Parametric modeling,
Design of Experiment

Corresponding author:

Yary Volpe
Tel.: +39-554796396
Fax.: +39-554796700
e-mail: yary.volpe@unifi.it
Address: via di Santa Marta, 3,
50139 Firenze

Abstract

Pneumatic spindles have been introduced in a wide range of industrial applications. In fact, air motors offer a cost effective alternative to conventional electric devices and often remarkable functional improvements. In spite of their growing diffusion, air motor design is still performed mainly according to companies' expertise, usually building a number of prototypes until the desired torque/speed (or power/speed) curve is obtained. The aim of this work is to provide a predictive model capable of estimating the characteristic curves by setting a set of air motor geometrical characteristics and inlet air pressure, in order to reduce the number of prototypes to be built. The presented study has been carried out with reference to vane motor, generally suitable for applications requiring high operating speeds. A statistical experimental approach (based on DoE technique) has been used in order to derive a mathematical-empirical model relating the geometrical and fluid-dynamic parameters with the system "response". The geometric parameters, defining the shape of the spindle, have been successively used to create a parametric CAD model with the corresponding technical drawings. The developed methodology, tested on a series of prototypes, proved to be effective in forecasting the characteristic curves of vane type air motor; moreover, due to the extremely low computational cost, it allows to assess a large number of design alternatives and to select the one best fitting the design target.

1 Introduction

Pneumatic motors have been widely recognized to be suitable for a number of industrial (and non industrial) applications such as robotics, automation, dental, etc. They often present considerable advantages when compared to electrical devices. For instance, they can be safely loaded until they stall and can be stopped, started and reversed continually without causing any damage, unlike their electrical counterpart. They are also highly effective at withstanding extreme heat, vibration and impact, making them ideal for use in particularly demanding applications, including those where it is impractical or unsafe to use electric motors (i.e. explosive and volatile atmospheres). Finally, compared to an electrical motor, a smaller air motor can deliver the same power avoiding in some cases the use of gearboxes for reducing its speed.

Pneumatic motors convert fluid-dynamic energy into mechanical energy. The power produced by a pneumatic motor is determined by the flow and pressure drop of the motor. The displacement and pressure drop of the motor determines the torque it generates. The power output is thus directly proportional to the speed.

Pneumatic motors can be classified into two main categories:

- volumetric motor;
- dynamic motor.

Generally, volumetric motors are characterized by closed spaces that, contracting and expanding while the motor runs, vary the volume.


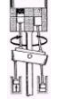


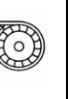
Dynamic motors, i.e. turbines, are based on the interaction between a high speed air flow and rotor blades [1].

The principal types of both volumetric and dynamic motors and their operating features are shown in Tab.1.

Rotary vane, gear-type, axial and radial-piston air motors are most commonly used for industrial applications. These designs operate with highest efficiency and longevity from lubricated air.

In particular, piston air motors [2,3,4] are used in applications requiring high power, high starting torque, and accurate speed control at low speeds. Gear-type motors are suitable for low

power and high speed. Turbine motors are used where very high speed but low starting torque is required. Finally, rotary vane motors [5,6] are used in applications requiring low to medium power outputs and high speed. The small external dimensions and the operating features, make vane motors particularly suitable to be used in pneumatic spindles. For these reasons vane motors are used in many industrial applications (e.g. milling, grinding, and drilling).

Characteristic	AIR MOTOR				
	VOLUMETRIC				DYNAMIC
	Radial-piston	Axial-piston	Vane motor	Gear-Type motor	Turbine
					
Power (kW)	1.5-3.0	1-6	0.1-18	0.5-5	0.01-0.2
Max. velocity (rpm)	6000	5000	30000	15000	120000
Max. expansion ratio	1:2	1:1.5	1:1.6	1:1	-
Num. of cylinders or vane per round	4-6	4	2-10	10-25	One stage

Tab. 1 Principal types of air motors (from [7] and [8]).

Since the present study has been carried out with reference to vane motors, their typical design and working principle is described below.

Vane motors have axial vanes fitted into radial slots running the length of a rotor, which is mounted eccentric with the bore of the motor's body housing (stator). During the start-up the vanes

are kept in contact with the stator inner walls by means of springs, cam action, or air pressure, depending on design.

The centrifugal force that develops when the rotor turns aids this sealing action. Torque develops from pressure acting on one side of the vanes.

The typical vane motor design is shown in Fig.1.

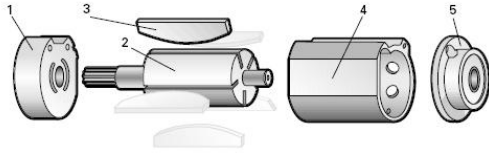


Fig. 1 Vane motor components: 1. Front end plate; 2. Rotor; 3. Vane; 4. Stator; 5. Rear end plate (from [9]).

The huge attention on these motors is evidenced by very interesting works concerning pneumatic spindles reported in the scientific literature. Naranjo et al. [10] developed a new small pneumatic motor as an alternative to electric motors for machining processes at small dimensions, with potential use in micromachines and microfactories. Mihajlov et al. [11] developed a new pneumatic rotary actuator with elastic chambers. Different prototypes of an air motor were developed by Nishi et al. in order to obtain new air driven actuator [12,13]. Pneumatic motors have been also used as actuators for different applications such as robots for pipe inspection [14].

In spite of their growing diffusion and the interest demonstrated by the scientific community, to the best of authors' knowledge, vane motor design is still performed mainly according to companies' expertise, usually building a number of prototypes until the desired torque/speed (or power/speed) curve is obtained.

This work is meant to investigate the possibility of developing a design tool capable to predict the performance of a vane motor and to provide the designer with an automatically updatable 3D model of the motor itself, together with all the necessary technical drawings.

2 Why DoE?

The mathematical theory describing the working principle of rotary vane motors is a well know one and relies on the ideal thermodynamic cycle shown in Fig. 2.

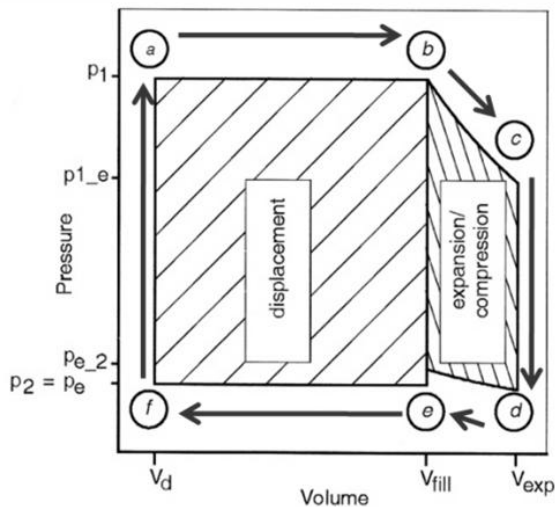


Fig. 2 Ideal thermodynamic cycle for a vane motor (from [8]).

It can be demonstrated that, when assuming a polytropic transformation and an ideal gas, the total work W is given by:

$$W = W_{\text{expansion}} + W_{\text{displacement}} + W_{\text{compression}} \quad (1)$$

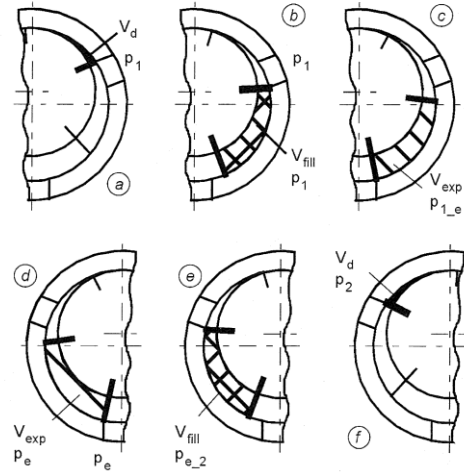


Fig. 3 Typical phases of vane motor cycle (from [8]).

Referring to Fig.3 and supposing that:

$$p_{1_e} = p_1 \left(\frac{V_{\text{fill}}}{V_{\text{exp}}} \right)^n \quad (2)$$

where $1.3 < n < 1.4$, it is possible to write:

$$W_{\text{expansion}} = - \int_c^b p \cdot dv = \frac{p_1 \cdot V_{\text{fill}}}{n-1} \cdot (\varepsilon^{1-n} - 1)$$

$$W_{\text{displacement}} = - \int_b^a p \cdot dv = (p_1 - p_2) \cdot (V_{\text{fill}} - V_d) \quad (3)$$

$$W_{\text{compression}} = - \int_e^d p \cdot dv = \frac{p_2 \cdot V_{\text{exp}}}{n-1} \cdot (\varepsilon^{n-1} - 1)$$

The expansion coefficient ε is defined as:

$$\varepsilon = \frac{V_{\text{exp}}}{V_{\text{fill}}} \quad (4)$$

In order to use the described approach to design a new device, the mathematical model must be generalized by taking into account "non idealities" such as:

- mechanical losses (mainly due to friction);
- fluid-dynamic losses (due to variable geometry ducts and real fluid behavior in intra-vane space);
- vane leakage.

These kinds of loss sources, however, are difficult to measure and, most important, are extremely difficult to correlate with operating and design parameters such as:

- inlet air condition;
- device geometry;
- material properties;
- device speed.

Some interesting works concerning the development of models to predict pneumatic torque/speed (or power/speed) curve have been reported in the literature. In particular, using geometrical data and the theory of thermodynamic processes, Beater [8,15] developed a model of an ideal reversible motor. Moreover, in his work, leakage paths and friction are added to describe the behavior of real motors.

Nevertheless these works usually refer to specific motor design, as a consequence they lack in general applicability and are very difficult to be effectively used in the design phase of a new device.

In this paper an alternative procedure based on DoE [16,17] is proposed in order to derive the characteristic torque-speed curve from a set of design and operating parameters.

2.1 DoE model

From the analysis of the ideal cycle (Fig. 2) and from what mentioned above about loss sources, it can be observed that work provided by the vane motor is strongly influenced by

expansion volume, inlet air pressure and pressure fall due to the inlet section.

Based on these considerations a first set of parameters was selected in order to model the motor behavior (i.e. torque C_m [Nm]):

- 1) stator inner diameter (D_s [mm]);
- 2) rotor diameter (D_r [mm]);
- 3) vane (rotor) length (L [mm]);
- 4) number of vanes (z);
- 5) inlet diameter (d_{in} [mm]);
- 6) outlet diameter (d_{out} [mm]);
- 7) inlet pressure (p_{in} [bar]);
- 8) rotating speed (n [rpm]).

Parameters from 1 to 6 are purely geometrical and are summarized in Fig. 4.

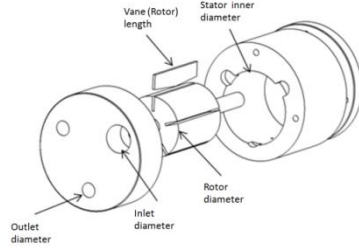


Fig. 4 Main geometric parameters.

On the basis of the listed parameters, the most obvious function which is to consider (to be determined by means of DoE technique) can be expressed as:

$$C_m = F(D_r, D_s, L, z, d_{in}, d_{out}, n, p_{in}) \quad (5)$$

In case the simplest experimental plan is supposed (2 levels per parameter), the function shown in eq. 5 involves a total of $2^8 = 256$ tests.

In order to reduce the experimental test number it is useful to observe that in practical cases (as demonstrated by commercial products technical sheets) torque vs. speed curve is a straight line. As a consequence, a new expression for torque can be written as follows:

$$C_m = m \cdot n + q \quad (6)$$

A further simplification has been achieved from observing that commercial products usually feature a 5 vane design. This has allowed to eliminate z from the design variables.

As a consequence, two new functions can be defined:

$$m = F_1(D_r, D_s, L, d_{in}, d_{out}, p_{in})$$

$$q = F_2(D_r, D_s, L, d_{in}, d_{out}, p_{in}) \quad (7)$$

Accordingly, a total of 64 tests are, now, necessary. Since inlet pressure p_{in} is not a geometric parameter, the required total number of prototypes for a full factorial plan is 32.

The final solution chosen in this work, in order to further reduce the number of prototypes and the overall experiment costs, was to select a V order fractional factorial ($2^{5-1} = 16$) and to replicate the experimental test with 2 levels of inlet pressure (i.e. 3; 4 bar), thus obtaining 2 set of values (m_1, q_1 and m_2, q_2) for the different pressure levels. The choice of the lowest pressure level was driven by the observation that, in practice, this kind of devices is seldom used with a pressure lower than 3 bar. The limitation of the higher pressure level has been set a-posteriori, due to the experimental setup which proved not to be reliable for rotation speeds higher than 25000 rpm.

The five geometric parameters defined in eq. 7 have been modified in order to avoid physically impossible configurations (e.g. rotor diameter lower than stator diameter). In particular two new parameters have been defined as follows:

1. $\%d_{in}$ defines the inlet diameter as a percentage of the outlet diameter (i.e. $d_{in} = \%d_{in} \cdot d_{out}$)
2. $\%e$ defines the eccentricity expressed as a percentage of the rotor diameter (i.e. $D_r = D_s \cdot (1 + 2 \cdot \%e)$)

The parameter values, considered in order to build the spindle prototypes for the experimental tests, are chosen on the basis of

technical specification of commercially available units. Selected dimensions are summarized in Tab. 2.

Model #	D_r	L	d_{out}	$\%d_{in}$	$\%e$
01	25	15	6,0	80	10
02	15	30	6,0	80	10
03	25	30	6,0	80	5
04	15	15	2,5	100	5
05	25	15	2,5	100	10
06	15	30	2,5	100	10
07	25	30	2,5	100	5
08	15	15	6,0	100	10
09	25	15	6,0	100	5
10	15	30	6,0	100	5
11	25	30	6,0	100	10
12	25	15	6,0	80	10
13	15	30	6,0	80	10
14	25	30	6,0	80	5
15	15	15	2,5	100	5
16	25	15	2,5	100	10

Tab. 2 Design parameters summary.

The typical form of the predictive equation estimated by means of experimental tests result to be:

$$\lambda = a_0 + a_1 \cdot D_r + a_2 \cdot L + a_3 \cdot d_{out} + a_4 \cdot \%d_{in} + a_5 \cdot \%e + a_6 \cdot D_r \cdot L + \dots$$

$$\dots + a_7 \cdot D_r \cdot d_{out} + a_8 \cdot D_r \cdot \%d_{in} + a_9 \cdot D_r \cdot \%e + a_{10} \cdot L \cdot d_{out} + a_{11} \cdot L \cdot \%d_{in} + \dots \quad (8)$$

$$\dots + a_{12} \cdot L \cdot \%e + a_{13} \cdot d_{out} \cdot \%d_{in} + a_{14} \cdot d_{out} \cdot \%e + a_{14} \cdot \%d_{in} \cdot \%e$$

where λ is alternatively m_1, m_2, q_1 or q_2 and a_i are the coefficients which are provided by using the software package Minitab 15[®].

2.2 Experimental set-up

The 16 prototypes were carefully characterized by using the test bench shown in Fig. 5.

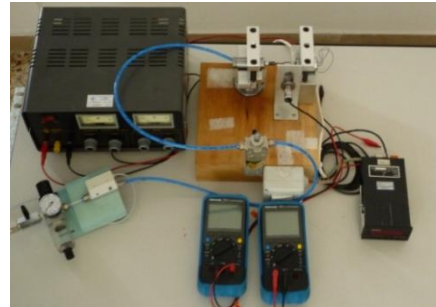


Fig. 5 Experimental set up.

The complete set of rotors are shown in Fig. 6, while four of the prototypes in Fig. 7.



Fig. 6 Rotors.



Fig. 7 Four of the tested prototypes.

The test bench consists of an air compressor capable of providing air with a pressure up to 10 bar, an air pressure regulator, a lubrication unit for adding lubricant (oil) to compressed air (in order to prevent early wear of vanes), a flow gauge, an optical rotational velocity meter and a dynamo used to vary the braking torque at different rotation speeds, connected, in its turn, to: a voltmeter, an ammeter and a rheostat.

The braking torque C_r , produced by the dynamo unit, can be evaluated using eq. 9.

$$C_r = \frac{K^2 \cdot \omega}{R + R_f} = \frac{K^2 \cdot \omega}{R + \frac{V}{I}} \quad (9)$$

Where:

- K = dynamo constant (which is known thanks to prior unit characterization);
- ω = rotation velocity;
- R = dynamo inner electrical resistance;
- R_f = resistance provided by the rheostat;
- V = potential difference between the two dynamo poles;
- I = current flowing through the dynamo.

The electrical scheme is shown in Fig. 8.

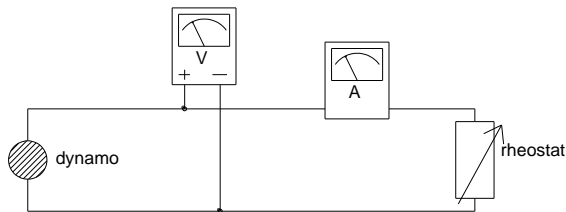


Fig. 8 Dynamo unit electrical connections.

The dynamo unit is connected to the spindle shaft by means of an elastic joint.

The described experimental set-up is used to determine the characteristic curve (torque vs. speed) of each spindle prototype.

More in detail, the spindle is supplied by compressed air (3 or 4 bar) and the rheostat resistance value is varied in order to obtain a 15 Hz step in frequency variation of the shaft rotation speed. Once the speed has stabilized, ω , V and I are recorded so that the corresponding torque can be computed. In order to increase robustness, the characteristic curve for each prototype and inlet pressure is evaluated 5 times.

As already stated characteristic curves of commercial spindles are straight lines; moreover this assumption has been taken into account when deriving the torque expression shown in eq. 6. A typical characteristic curve is shown in Fig. 9 (the best fit linear regression is superimposed on the experimental data).

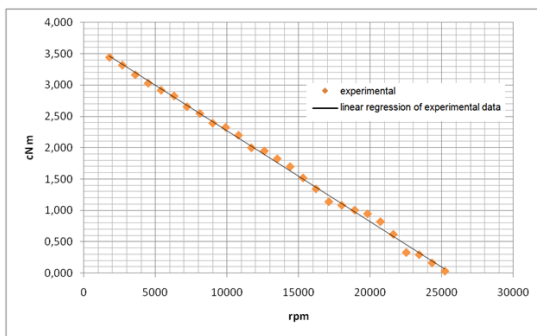


Fig. 9 Typical torque-speed curve. Experimental data (◊) and linear regression (-).

2.3 Results

As already anticipated the DoE analysis has been performed using Minitab 15[®]. Main effects and interactions contributions are shown in the Pareto chart of Fig. 10 which refers to the m_1 (3 bar) coefficient.

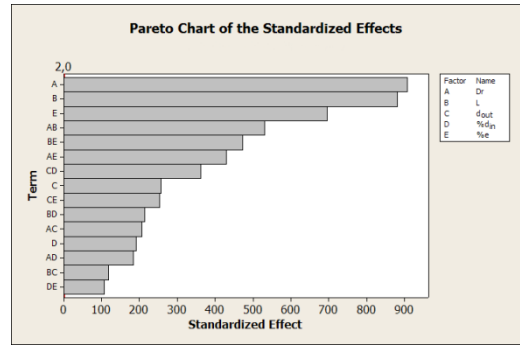


Fig. 10 Pareto chart of m_1 coefficient.

The main effect plot for the same coefficient is also provided in Fig. 11.

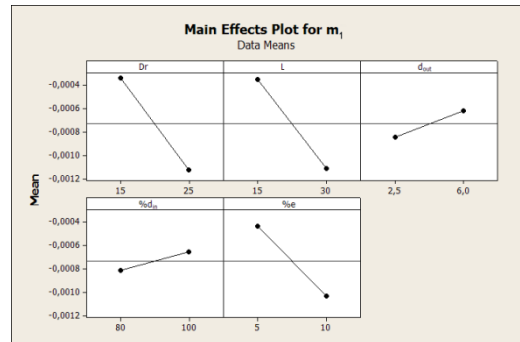


Fig. 11 Main effects plot of m_1 coefficient.

By observing Figs. 10 and 11, it is possible to state that the three most relevant parameters affecting the slope of the characteristic curve are: rotor diameter, vane length and eccentricity.

The same parameters appear to be the most relevant for all the other coefficients (q_1, m_2, q_2).

2.4 Validation

In order to validate the mathematical models, a new set of five spindle prototypes, different from the ones used for developing DoE models, has been considered. The characteristic torque vs. speed curves (for both 3 and 4 bar inlet pressure), estimated by the predictive equation (eq. 6), have been compared with the ones experimentally measured using the test bench.

In Figs. 12 and 13 are graphically shown the comparisons between the experimental characteristic curves (obtained by means of linear regression applied to experimental data) and the ones coming from the predictive equations for two of the validation prototypes (3 bar inlet pressure). In the same Figures the validation prototype parameters ($D_r, L, d_{out}, \%d_{in}, \%e$), the relative percent errors between experimental and estimated values and respective analytical characteristic curve coefficients are illustrated.

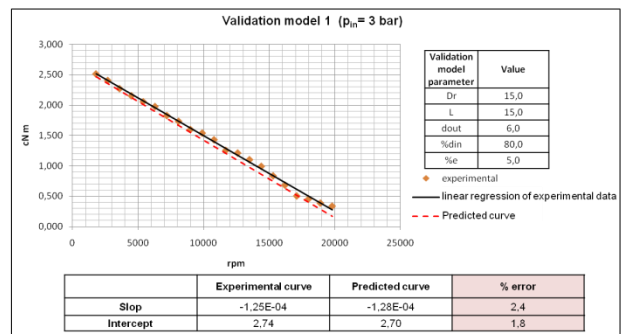


Fig. 12 Experimental and estimated characteristic curve comparison for validation model n.1.

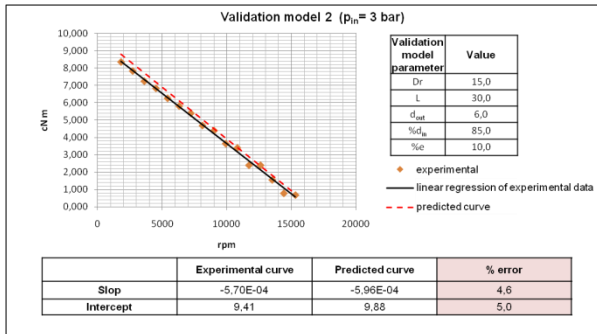


Fig. 13 Experimental and estimated characteristic curve comparison for validation model n.2.

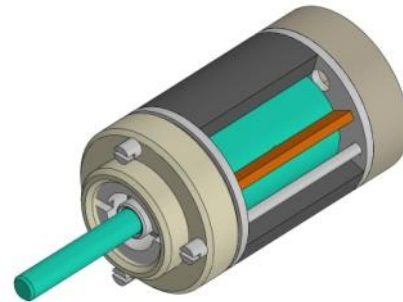


Fig. 14 3D parametric model (D_r = 15 mm; L = 30; d_{out} = 6; %d_{in}=80; %e=10)

The percent error, of both slope and intercept, is not greater than 5% for each of the 5 validation models. Thus, based on these results, the predictive models can be considered to accurately reproduce the real behaviour of spindles in terms of torque-speed curve.

The obtained models can be effectively used to predict the performance of a new spindle, once a set of design parameters is provided. Due to the very simple mathematical expression, the computation time necessary to build the predicted characteristic curve is negligible.

3 Design tool development

In order to further reduce the time required to design new spindles, a software tool has been developed using Matlab®. Such a tool features a Graphical User Interface (GUI) where the design variables can be input and the resulting characteristic curves (torque-speed, power-speed) are shown. The analytical curves are computed using the predictive equations described in section 2. The GUI is directly interfaced with an Excel spreadsheet, where the design variables are stored and successfully used as input to drive the parameters of an appositely built parametric CAD model of the spindle.

3.1 Parametric Model

The parametric spindle model has been built using Autodesk Inventor® 2008.

The 3D model and the 2D drawing of the assembly for two different spindles are shown respectively in Fig. 14 and Fig. 15.

As anticipated, the design parameters, linked to CAD model dimensions, are stored in an Excel spreadsheet which, in its turn, is compiled through the GUI.

The set of design parameters is divided into 2 sub-sets:

- Primary design variables (the ones which directly affect the spindle's characteristic curves):
 - rotor diameter (D_r [mm]);
 - vane (rotor) length (L [mm]);
 - outlet diameter (d_{out} [mm]);
 - inlet diameter (as a percentage of the outlet diameter %d_{in});
 - eccentricity (as a percentage of the rotor diameter %e).
- Secondary design variables (the ones not directly affecting spindle performance but which are necessary to define overall design):
 - spindle outer diameter;
 - bearing inner diameter;
 - bearing outer diameter;
 - bearing axial dimension;
 - vane thickness;
 - rear and front spacers thickness (see Fig. 15);
 - screw diameter.

Some of the secondary design variables (e.g. outer diameter, screw diameter) are obviously related to spindle stiffness and resistance, while others (e.g. bearing dimensions) depend on the available dimensions of commercial devices.

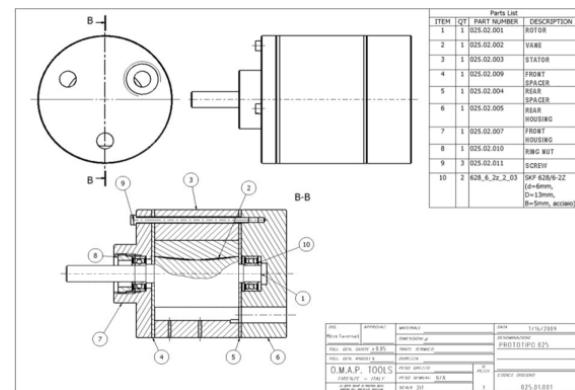


Fig. 15 3D parametric model (D_r = 15 mm; L = 15; d_{out} = 2.5; %d_{in}=100; %e=5)

3.2 GUI

The Graphical User Interface is shown in Fig. 16. Primary and secondary variables are split into two different interface areas.

The GUI is additionally provided with two graphical windows showing, respectively, the torque-speed and power-speed curves (since torque-speed curve is a negative slope line, the power-speed curve is a parabola).

General usage procedure consists of:

- 1) setting primary and secondary variables;
- 2) generating characteristic curves;
- 3) checking the suitability of the obtained curves to the design objective;
- 4) iterating steps 1 to 3 until the objective is matched;
- 5) generating the correspondent 3D CAD models and technical drawings for final validation.

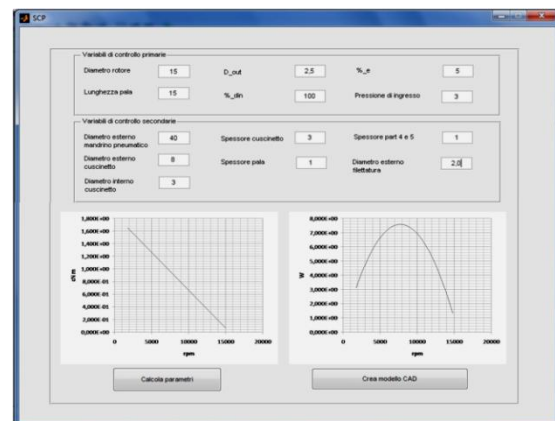


Fig. 16 Graphical User Interface

4 Conclusion and future work

A predictive tool capable of estimating the characteristic curves of pneumatic spindles, based on rotary vane architecture, has been developed.

The tool requires, as input, a set of design variables describing the spindle geometry. Such a tool is based on a simple mathematical model obtained by means of Design of Experiment technique which involved a set of 16 prototypes. The model has been validated by means of experimental analysis carried out on 5 additional devices; the good agreement between predicted and actual curves demonstrates the reliability and the accuracy of the developed tool.

A Graphical User Interface has been developed in order to facilitate the usage of the described tool. Additionally the design variables directly input in the GUI have been linked to a parametric CAD model of the spindle, which is automatically updated, together with the corresponding technical drawings, when a new set of variables is provided.

The developed tool, due to the extremely low computational cost, allows to assess a large number of design alternatives and to select the one best fitting the design target in terms of performance. Thereby it proves to be extremely effective in reducing the number of prototypes to be built when developing a new spindle design.

Future work will be addressed to enhance the prediction capabilities of the proposed tool by increasing the number of design variables simultaneously taken into account. Moreover, the possibility of using an optimization algorithm capable to automatically determine spindle parameters on the basis of a user-provided characteristic curve will be investigated.

Acknowledgments

The authors wish to thank Dr. Mirco Tavernari for his valuable contribution related to DoE implementation and result processing.

References

- [1] G. Belforte. *Manuale di Pneumatica*, Tecniche Nuove
- [2] RW. Dunlop. *Development of pneumatic devices to provide integrated motion control using oil-free air*. In Conference Proceedings 8th International Symposium on Fluid Power, Paper B1, April 19–21, 1989; Birmingham, p. 87–106.
- [3] HM. Mahgoub, IA. Craighead. *Robot actuation using air motors*. In Int. J. Adv Manuf Technol 1996;11:221–9.
- [4] M.O. Tokhi, I. N. Reynolds, M. Brisland. *Real-time control of a radial piston air motor*. In Conference Proceedings 15th Triennial World Congress, 2002; Barcelona (Spain).
- [5] DJ. Saunders. *Rotary air vane motors: their use as a drive medium*. In Hydraul Pneum Mech Power, 1978;24(280):175–8.
- [6] S. Yu-Ta, H. Yean-Ren, *Design and implementation of an air-powered motorcycles*. In Applied Energy, 2009, 86: 1105–1110.
- [7] www.hydraulicspneumatics.com.
- [8] P. Beater. *Pneumatic drives: system design, modelling and control*, Springer, 2007, XIV, p. 244, ISBN: 978-3-540-69470-0.
- [9] www.atlascopco.com.
- [10] J. Naranjo, E. Kussul, G. Ascanio, *A new pneumatic vanes motor*. In Mechatronics 20, 2010, 424–427.
- [11] M. Mihajlov, O. Ivlev, A. Gräser. *Dynamics and control of a two-link robot arm with soft fluidic actuators for assistance and service applications*. VDI Berich 2008; 2012:41–4.
- [12] A. Nishi, Y. Zhang, H. Miyagi, CS. Yang. *Development of low pressure air driven actuator*. In Proceedings of JSME Annual Conference on Robotics and Mechatronics, June, 1997; Tokyo, Japan, p. 163–4.
- [13] A. Nishi, Y. Zhang, *Low-pressure air motor for wall-climbing robot actuation*, Mechatronics 13 (2003) 377–392.
- [14] K. Suzumori, K. Hory, T., Miyagawa . *A direct-drive pneumatic stepping motors for robots: design for pipe inspection microrobots and human-care robots*. In Proceedings of the IEEE international conference on robotics and automation; 1998. p. 3047–52.
- [15] P. Beater. *Modelling and control of pneumatic vane motors*. In Int. J. Fluid Power, 2004;5:7–16.
- [16] D.C. Montgomery. *Design and analysis of experiments*. John Wiley & Sons, New York.
- [17] A. Jiju, *Design of Experiments for Engineers and Scientists*, BH.